Ang-2/VEGF bispecific antibody reprograms macrophages and resident microglia to anti-tumor phenotype and prolongs glioblastoma survival

Dual inhibition of Ang-2 and VEGF receptors normalizes tumor vasculature and prolongs survival in glioblastoma by altering macrophages

Teresa E. Peterson[a,b,1,2], Nathaniel D. Kirkpatrick[a,1,3], Yuhui Huang[a,1,4], Christian T. Farrar[c], Koen A. Marijt[a,5], Jonas Kloepper[a], Meenal Datta[a,d], Zohreh Amoozgar[a], Giorgio Seano[a], Keehoon Jung[a], Walid S. Kamoun[a,6], Trupti Vardam[a,7], Matija Snuderl[a,8], Jermaine Goveia[a,9], Sampurna Chatterjee[a], Ana Batista[a,10], Alona Muzikansky[e], Ching Ching Leow[f], Lei Xu[a], Tracy T. Batchelor[g], Dan G. Duda[a], Dai Fukumura[a,11], and Rakesh K. Jain[a,11]

[a]Edwin L. Steele Laboratories, Department of Radiation Oncology, Massachusetts General Hospital and Harvard Medical School, Boston, MA 02114; [b]Department of Biological Chemistry and Molecular Pharmacology, Harvard University, Boston, MA 02115; [c]Athinoula A. Martinos Center for Biomedical Imaging, Massachusetts General Hospital and Harvard Medical School, Charlestown, MA 02129; [d]Department of Chemical and Biological Engineering, Tufts University, Medford, MA 02155; [e]Biostatistics Center, Massachusetts General Hospital and Harvard Medical School, Boston; MA 02114; [f]Department of Translational Medicine Oncology, MedImmune, Gaithersburg, MD 20878; and [g]Stephen E. and Catherine Pappas Center for Neuro-Oncology, Department of Neurology, Massachusetts General Hospital and Harvard Medical School, Boston, MA 02114

Contributed by Rakesh K. Jain, December 29, 2015 (sent for review December 2, 2015; reviewed by James W. Hodge and Balveen Kaur)

Glioblastomas (GBMs) rapidly become refractory to anti-VEGF therapies. We previously demonstrated that ectopic overexpression of angiopoietin-2 (Ang-2) compromises the benefits of anti-VEGF receptor (VEGFR) treatment in murine GBM models and that circulating Ang-2 levels in GBM patients rebound after an initial decrease following cediranib (a pan-VEGFR tyrosine kinase inhibitor) administration. Here we tested whether dual inhibition of VEGFR/Ang-2 could improve survival in two orthotopic models of GBM, Gl261 and U87. Dual therapy using cediranib and MEDI3617 (an anti–Ang-2–neutralizing antibody) improved survival over each therapy alone by delaying Gl261 growth and increasing U87 necrosis, effectively reducing viable tumor burden. Consistent with their vascular-modulating function, the dual therapies enhanced morphological normalization of vessels. Dual therapy also led to changes in tumor-associated macrophages (TAMs). Inhibition of TAM recruitment using an anti–colony-stimulating factor-1 antibody compromised the survival benefit of dual therapy. Thus, dual inhibition of VEGFR/Ang-2 prolongs survival in preclinical GBM models by reducing tumor burden, improving normalization, and altering TAMs. This approach may represent a potential therapeutic strategy to overcome the limitations of anti-VEGFR monotherapy in GBM patients by integrating the complementary effects of anti-Ang2 treatment on vessels and immune cells.

anti-angiogenic therapy | tumor microenvironment | tumor immunity | colony-stimulating factor 1 | macrophage

Glioblastoma (GBM) is the most common and aggressive primary malignant brain tumor in adults (1). Based on promising phase II trials, bevacizumab (Avastin), a VEGF monoclonal antibody, was approved by the Food and Drug Administration in 2009 as salvage monotherapy for recurrent GBM (rGBM) (1–5). However, three randomized phase III trials of bevacizumab in combination with chemoradiation in newly diagnosed GBM patients and in combination with chemotherapy in rGBM patients failed to prolong overall survival despite the extension of progression-free survival (6–8). A randomized trial of cediranib, a pan-VEGF receptor (VEGFR) tyrosine kinase inhibitor, with or without lomustine also failed to show improved survival in patients with rGBM (9). Inhibition of VEGFR2 transiently "normalized" GBM vasculature and improved the outcome of radiotherapy in mice bearing GBM (10). Vascular normalization also reduced intracranial edema, contributing to the survival benefit in animal models (11). Similarly, treatment with cediranib induced transient vessel normalization in patients with rGBM, effectively reducing edema (12, 13). Unfortunately, resistance to anti-VEGF therapy develops rapidly in patients with GBM. Modulation of other angiogenic, growth, and survival programs in

Significance

Inhibition of the VEGF/VEGF receptor (VEGFR) pathway has failed to increase overall survival in phase III trials in patients with glioblastoma (GBM). Previously we identified the angiopoietin-2 (Ang-2)/TEK receptor tyrosine kinase (Tie-2) pathway as a potential driver of resistance to VEGF inhibition in GBM. Here we show that dual inhibition of VEGFRs and Ang-2 inhibits tumor growth and prolongs vessel normalization compared with VEGFR inhibition alone, resulting in improved survival in murine GBM models. Furthermore, by blocking macrophage recruitment, we demonstrate that macrophages contribute to the beneficial effects of dual therapy.

Author contributions: T.E.P., N.D.K., Y.H., C.T.F., K.A.M., J.K., M.D., Z.A., K.J., W.S.K., T.V., M.S., J.G., S.C., C.C.L., L.X., T.T.B., D.G.D., D.F., and R.K.J. designed research; T.E.P., N.D.K., Y.H., C.T.F., K.A.M., J.K., M.D., Z.A., W.S.K., T.V., M.S., J.G., S.C., A.B., and L.X. performed research; T.E.P., N.D.K., Y.H., C.T.F., K.A.M., J.K., M.D., Z.A., G.S., K.J., W.S.K., T.V., M.S., J.G., S.C., A.B., and A.M. analyzed data; and T.E.P., N.D.K., Y.H., J.K., M.D., Z.A., G.S., K.J., T.V., J.G., L.X., T.T.B., D.G.D., D.F., and R.K.J. wrote the paper.

Reviewers: J.W.H., Center for Cancer Research, National Cancer Institute; and B.K., Comprehensive Cancer Center, The Ohio State University.

Conflict of interest statement: R.K.J. received consultant fees from Ophthotech, SPARC, SynDevRx, and XTuit. R.K.J. owns equity in Enlight, Ophthotech, SynDevRx, and XTuit and serves on the Board of Directors of XTuit and on the Boards of Trustees of Tekla Healthcare Investors, Tekla Life Sciences Investors, Tekla Healthcare Opportunities Fund, and Tekla World Healthcare Fund. No reagents or funding from these companies was used in these studies. T.T.B. received consultant fees from Merck, Roche, Kirin Pharmaceuticals, Spectrum Pharmaceuticals, Novartis, and Champions Biotechnology. C.C.L. is an employee of MedImmune.

Freely available online through the PNAS open access option.

[1]T.E.P., N.D.K., and Y.H. contributed equally to this work.

[2]Present address: Wilson Sonsini Goodrich & Rosati, Palo Alto, CA 94304.

[3]Present address: Novartis Institutes for BioMedical Research, Inc., Cambridge, MA 02139.

[4]Present address: Cyrus Tang Hematology Center, Soochow University, Suzhou 215123, People's Republic of China.

[5]Present address: Department of Clinical Oncology, Leiden University Medical Center, 2333, Leiden, The Netherlands.

[6]Present address: Merrimack Pharmaceuticals, Cambridge, MA 02139.

[7]Present address: Department of Immunology, College of Medicine, Mayo Clinic, Scottsdale, AZ 85259.

[8]Present address: New York University Langone Medical Center and Medical School, New York, NY 10016.

[9]Present address: Department of Oncology, Vesalius Research Center, KU Leuven, B-3000 Leuven, Belgium.

[10]Present address: Trends in Cancer, Cambridge, MA 02139.

[11]To whom correspondence may be addressed. Email: dai@steele.mgh.harvard.edu or jain@steele.mgh.harvard.edu.

This article contains supporting information online at www.pnas.org/lookup/suppl/doi:10.1073/pnas.1525349113/-/DCSupplemental.

response to VEGF-signaling blockade may mediate this resistance (1, 14–16). Thus, there is an urgent need to develop novel combinations targeting such resistance pathways to increase survival in GBM.

Angiopoietin-2 (Ang-2) is often up-regulated in GBMs (17–19) and is thought to play a role in GBM angiogenesis (17, 20, 21). Ang-2 is a member of the angiopoietin family that signals primarily through the tyrosine kinase receptor TEK receptor tyrosine kinase (Tie-2). Ang-1 and Ang-2 play important, often complementary, roles in maintaining normal vasculature through the modulation of vessel stability (22). Ang-2–mediated vessel destabilization can be either pro- or antiangiogenic in a context-dependent manner (17, 23–26). Increased Ang-2 expression may be an escape mechanism to anti-VEGF therapy. In both clinical and preclinical GBM studies, Ang-2 levels decline temporarily following inhibition of the VEGF pathway but later rebound as tumors become resistant to therapy (10, 12). We have shown that ectopic expression of Ang-2 in a GBM animal model compromised the survival benefit of VEGF-signaling inhibition by impairing vessel normalization and edema control (27). Moreover, tumor autopsy tissues from rGBM patients treated with anti-VEGF therapy showed abnormally high levels of Ang-2 (28), and the Ang-1/Ang-2 ratio correlated positively with survival (29) and vascular normalization (12). Therefore, we hypothesized that dual inhibition of VEGF and Ang-2 signaling could prolong the window of normalization or normalize vessels to a greater extent and thereby enhance the survival benefit of anti-VEGF therapy.

Additionally, we recently demonstrated that vascular normalization leads to efficient immune cell recruitment and promotes an immuno-stimulatory microenvironment in murine breast tumors (30). Given that tumor-associated macrophage (TAM) infiltration is an important determinant of tumor progression and response to therapy in GBM and other tumors (31–33), we further hypothesized that TAMs may play a role in the response to dual therapy.

In this study we combined an Ang-2–neutralizing monoclonal antibody that targets both human and murine Ang-2, MEDI3617 (MedImmune) (34), with cediranib (AstraZeneca Pharmaceuticals) and assessed the effects of dual therapy on survival, tumor growth, vascular normalization, and TAM phenotype in two orthotopic models of GBM in mice: Gl261 (a syngeneic, hypovascular murine GBM model) and U87 (a highly angiogenic human GBM model).

Results

Dual Anti-VEGFR/Ang-2 Therapy Extends Survival Compared with Cediranib Monotherapy. We treated mice bearing orthotopic Gl261 or U87 tumors with control IgG, MEDI3617, cediranib, or cediranib+MEDI3617 dual therapy. Consistent with our previous experience in GBM (10, 11, 27), treatment with cediranib alone significantly increased survival of Gl261-bearing mice compared with control (median 24 d vs. 20 d). MEDI3617 treatment also increased median survival (24 d). Strikingly, dual therapy significantly prolonged survival compared with the monotherapy and control arms (38 d) (Fig. 1*A* and Table S1). Similarly, dual therapy significantly increased mouse survival in U87-bearing mice (median 26 d) compared with mice treated with cediranib alone (13 d), MEDI3617 alone (7 d), or control treated mice (5 d) (Fig. 1*E* and Table S1).

Given the significant improvement in survival in mice treated with dual therapy over cediranib monotherapy, we next examined the impact of treatment on tumor growth. Gl261 tumors treated with either cediranib or dual therapy grew significantly more slowly than control tumors. Moreover, tumors treated with dual therapy grew more slowly than cediranib-treated tumors (Fig. 1*B*). This sustained delay in growth resulted in significantly smaller tumors near the median survival time of cediranib-treated mice (day 20) in the dual-therapy group compared with the cediranib group as measured by MRI (Fig. 1*C*). We also examined the extent of necrosis and observed no significant difference between Gl261 tumors treated with dual therapy or with cediranib

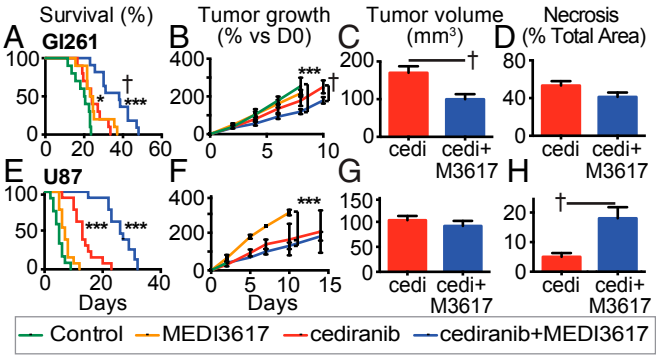

Fig. 1. Dual cediranib+MEDI3617 therapy enhances survival and reduces tumor burden in Gl261 and U87 tumors compared with cediranib therapy alone. Mice bearing Gl261 (*A–D*) or U87 (*E–H*) tumors were treated with control (green traces), MEDI3617 (orange traces), cediranib (red traces/bars), or dual therapy (blue traces/bars). (*A*) In Gl261 tumors, both cediranib and MEDI3617 monotherapies led to significantly higher overall median survival (24 d) than control treatment (20 d) (cediranib $*P = 0.017$; MEDI3617 $*P = 0.011$; $n = 10$). Dual therapy ($n = 11$) led to a significantly higher median survival (38 d) than control ($***P < 0.0001$) or cediranib treatment ($^{\dagger}P = 0.002$). (*B*) There was a significant difference in the growth rate of tumors treated with dual therapy compared with both control-treated ($***P < 0.0001$) and cediranib-treated ($^{\dagger}P = 0.0076$) tumors as measured by OFDI. (*C*) Dual therapy-treated tumors were significantly smaller than cediranib-treated tumors at day 20 as measured by MRI ($^{\dagger}P = 0.0089$). (*D*) There was no change in the extent of necrosis at day 20 ($P = 0.11$). (*E*) In the U87 model, both cediranib and dual therapy-treated mice had a significantly higher overall median survival (26 d and 13 d, respectively; $n = 13$) than control-treated mice (5 d; $n = 12$; $***P < 0.0001$). (*F* and *G*) There was no difference in tumor growth (*F*) or volume (*G*) between dual therapy-treated tumors and cediranib-treated tumors in the U87 model. (*H*) There was a significant increase in ischemic hypoxic changes (early necrosis) in dual therapy-treated tumors compared with cediranib-treated tumors at day 6 ($^{\dagger}P = 0.030$). cedi, cediranib; cedi+M3671, cediranib+MEDI3617. Error bars represent the SEM. $*P < 0.05$, $**P < 0.01$, $***P < 0.001$ compared with control unless otherwise indicated.

monotherapy (Fig. 1*D* and Fig. S1). Thus, dual therapy delayed GBM progression by slowing the tumor growth rate, resulting in a lower viable tumor burden in Gl261-bearing mice treated with dual therapy than in mice treated with cediranib monotherapy.

Interestingly, there was no detectable difference in the growth rate of U87 tumors treated with cediranib monotherapy or dual therapy (Fig. 1 *F* and *G*), suggesting that the inhibition of tumor growth was not a chief cause of the observed survival benefit. This finding is consistent with our previous study in the same tumor model (11). However, we detected a striking increase in areas of diffuse hypoxic ischemic change (i.e., early necrosis) (Fig. S1) by day 6 in the dual therapy-treated tumors as compared with both cediranib- and control-treated tumors (Fig. 1*H* and Fig. S2), resulting in a decreased viable tumor burden in mice treated with dual therapy.

Direct antiproliferative effects were observed in vitro with high concentrations of cediranib ($>10^3$ nM), but MEDI3617 had no effect on cell viability in either Gl261 or U87 tumors (Fig. S3). However, histological analyses of tumor apoptosis and proliferation did not reveal significant changes (Fig. S4) in either U87 or Gl261 tumors, suggesting that alternative mechanisms are responsible for reduced viable tumor burden.

Dual Therapy Enhances Normalization in Gl261 Tumors Compared with Cediranib Monotherapy. To determine the effects of cediranib+MEDI3617 dual therapy on the tumor vasculature, we assessed vessel morphology. In Gl261 tumors we focused our analysis on day 14 (the time point of the beginning of the end of cediranib-induced vascular normalization based on our preliminary studies) and day 21 (near the median survival of cediranib-treated mice) to

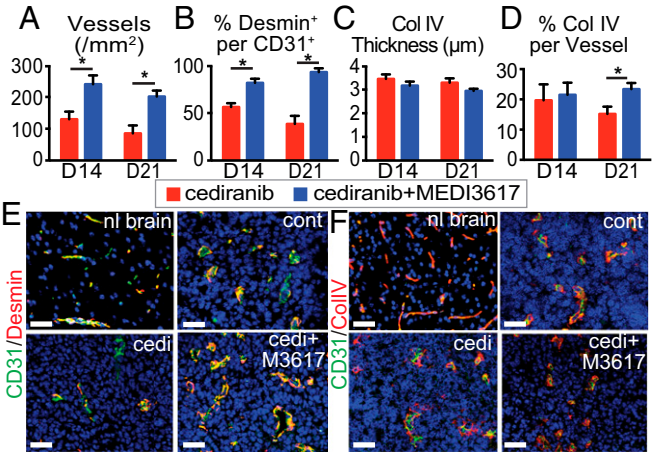

Fig. 2. Dual cediranib+MEDI3617 therapy extends vascular normalization in viable tissue compared with cediranib therapy alone. Gl261 tumors were collected from mice treated with cediranib (red bars) or dual therapy (blue bars) at days 14 or 21 after beginning treatment. Sections were stained for CD31 (for vessels), desmin (for perivascular cells), or collagen IV (for BM) and DAPI (for nuclei). (*A*, *B*, *D*) Both MVD (*A*) and perivascular cell coverage (the percentage of the desmin/CD31 double-positive area in the $CD31^+$ area) (*B*) were higher in the dual therapy-treated tumors than in cediranib-treated tumors at days 14 and 21, but BM coverage (*D*) was higher only at day 21. (*C*) There was no significant difference in BM thickness among groups. (*E*) Representative images of CD31 (green)/desmin (red) staining in the normal brain (nl brain) and in control (cont)-, cediranib (cedi)-, and dual therapy (cedi+M3617)-treated tumors on day 21. (*F*) Representative images of CD31 (green)/collagen IV (red) staining. Error bars represent the SEM. $*P <$ 0.05 compared with control unless otherwise indicated. (Scale bars, 50 μm.)

identify the effects of prolonged dual therapy compared with cediranib monotherapy. Tumor microvessel density (MVD) and perivascular cell coverage were higher in the dual therapy group than in cediranib-treated tumors at day 14, but there were no differences in the extent of basement membrane (BM) coverage or thickness (Fig. 2). By day 21, tumor vessels were still structurally normalized, with significantly higher BM coverage, in the mice treated with dual therapy (Fig. 2). Overall the vessels in the dual therapy-treated tumors had a more normalized vessel structure than the vessels in the cediranib-treated tumors (Fig. 2 *E* and *F*).

Because dual therapy induced sustained structural vessel normalization in Gl261, we next investigated whether these changes could translate to improved edema control. In addition to determining intratumoral edema, we assessed edema in both the ipsilateral hemisphere (to measure peritumoral edema) and the contralateral hemisphere (as a control for global changes in edema). In Gl261 tumors, both cediranib and dual therapy decreased edema in the ipsilateral and contralateral hemispheres compared with controls, although only cediranib had a statistically significant effect (Fig. 3 *A* and *B*; dual therapy $P = 0.052$). There was no difference among the treatment groups in edema within the tumor itself (Fig. 3*C*). These data suggest that edema control is not the major consequence of the improved normalization in dual therapy-treated tumors compared with cediranib-treated tumors.

Dual Therapy Improves Structural Vessel Normalization in U87 Tumors Compared With Cediranib Monotherapy. Vessels were analyzed at days 3 and 8 after treatment initiation to determine the effects of therapy during the previously defined time window of normalization (days 3–8) (10, 11, 27). Tumors treated with either cediranib alone or dual therapy displayed a significant decrease in MVD and BM thickness, but not BM coverage, at day 3 compared with control tumors (Fig. 4 *A*, *C*, *D*, and *F*). Perivascular cell coverage was significantly higher in dual therapy-treated tumors than in vessels from control- and cediranib-treated tumors (Fig. 4 *B* and *E*), suggesting a greater extent of vessel normalization after dual therapy. Indeed, after dual therapy GBM vessels exhibit better normalization (Fig. 4 *E* and *F*). These features were maintained in both the cediranib- and dual therapy-treated tumors at day 8. Notably, no control mice survived to day 8. MEDI3617 monotherapy induced some features of vessel normalization but did so in an inconsistent manner: Although there was no change in the MVD of MEDI3617-treated tumors, BM thickness was decreased compared with control tumors at day 3, and perivascular cell coverage was increased at day 8 (Fig. 4). Thus, as in Gl261 tumors, improved vascular normalization was observed in dual therapy-treated U87 tumors compared with cediranib-treated tumors. We also found that, as in Gl261 tumors, this vessel normalization with dual therapy did not translate into better edema control than seen with cediranib monotherapy (Fig. S5).

Dual Therapy Alters TAM Polarization. We recently demonstrated that the normalization of tumor vasculature leads to efficient immune cell recruitment and polarization of TAMs to antitumor phenotypes (30). Furthermore, Ang-2 blockade recently has been shown to improve tumor cell immune destruction (35). Based on these data we assessed whether immune cell infiltration or polarization might be altered by dual therapy in Gl261 tumors at day 10 (when tumors treated with dual therapy began to show significant delay in tumor growth as compared with tumors treated with cediranib monotherapy) (Fig. 1*B*). We found that the proportion of $F4/80^+$ TAMs was significantly changed among treatment groups (Fig. 5*A*). We further determined the phenotype of the TAMs using the M1 activation marker CD11c and the M2 activation marker MRC1. Fig. 5*B* and Fig. S6 show representative images of the gating strategy used to define TAM phenotypes. Although there was no difference among the treatment groups in either $CD11c^+MRC1^-$ M1-like TAMs (Fig. 5*C*) or $CD11c^-MRC1^+$ M2-like TAMs (Fig. 5*D*) alone, there were significantly more TAMs that did not display a clear M1- or M2-like activation state, i.e., $CD11c^+MRC1^+$ M1–M2 intermediate TAMs, in MEDI3617-treated tumors than in cediranib- and dual-treated tumors (Fig. 5*E*). We detected no significant change in the proportion of other immune cell populations [$CD8^+$ T cells, $CD4^+$ T cells, and $CD11b^+Gr1^+$ myeloid-derived suppressor cells (MDSCs)] (Fig. S7). Moreover, in vitro peritoneal macrophage stimulation studies showed enhanced expression of the M1-assocated genes such as *Cxcl9, Cxcl11*, and *Tnfα* with dual therapy (Fig. S8). Together, these results indicate that cediranib and MEDI3617 may have differential effects on TAM recruitment and phenotype.

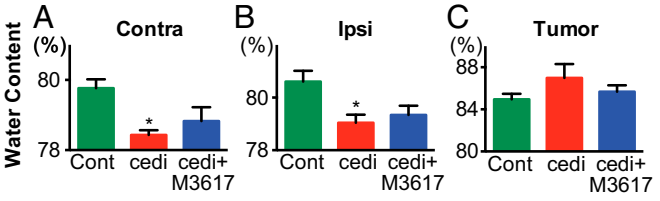

Fig. 3. Dual cediranib+MEDI3617 therapy promotes edema control in Gl261 tumors. Gl261-bearing mice ($n = 5$–7) were treated with control (green bars), cediranib (red bars), or dual therapy (blue bars). Water content (edema) was measured on day 10 after treatment start by wet/dry weight ratio in the contralateral hemisphere (Contra) (*A*), ipsilateral hemisphere (Ipsi) (*B*), and tumor (*C*). Cediranib monotherapy significantly decreased water content in both the contralateral ($P = 0.029$) and ipsilateral ($P = 0.024$) hemispheres. Dual therapy also decreased water content compared with control-treated tumors, although the decrease did not reach statistical significance (contralateral $P = 0.095$; ipsilateral $P = 0.052$). There was no significant difference in edema in any of the tissues treated with dual therapy as compared with cediranib treatment. cedi, cediranib; cedi+M3617, cediranib+MEDI3617; Cont, control. Error bars represent the SEM. $*P < 0.05$ compared with control unless otherwise indicated.

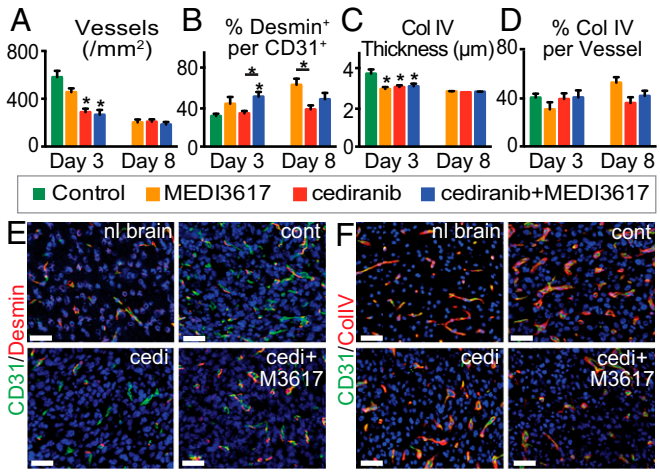

Fig. 4. Dual cediranib+MEDI3617 therapy improves vessel normalization in U87 tumors as compared with cediranib monotherapy. U87 tissues were collected from mice treated with control (green bars), MEDI3617 (orange bars), cediranib (red bars), or dual cediranib+MEDI3617 (blue bars) therapy at days 3 or 8 after beginning treatment. Sections were stained for CD31, either desmin or collagen IV (BM), and DAPI. (*A* and *C*) Both MVD (*A*) and BM thickness (*C*) were significantly decreased at day 3 by both cediranib and dual therapy as compared with control treatment and remained low at day 8. (*B*) In the dual therapy-treated tumors, perivascular cell coverage (the percentage of the desmin/CD31 double-positive area in the CD31$^+$ area) also was significantly higher on day 3 as compared with control tumors. (*D*) There was no significant difference in BM coverage among groups. (*E*) Representative images of CD31 (green)/desmin (red) staining in the normal brain (nl brain) and in control (cont)-, cediranib (cedi)-, and dual therapy (cedi+M3617)-treated tumors. (*F*) Representative images of CD31 (green)/collagen IV (red) staining in the normal brain and in control-, cediranib-, and dual therapy-treated tumors. Error bars represent the SEM. *$P < 0.05$ compared with control unless otherwise indicated. (Scale bars, 50 μm.)

The Survival Benefit of Dual Anti-VEGFR/Ang-2 Therapy Is Mediated by TAMs. To assess a causal role of TAMs in response to dual therapy, we used an anti–colony-stimulating factor-1 (CSF-1)–neutralizing antibody to block the recruitment of TAMs in Gl261 tumors (Fig. S9). CSF-1 blockade as a monotherapy or in combination with MEDI3617 or cediranib had no significant effect on survival (Fig. 6 and Fig. S10). However, when combined with the dual therapy it significantly compromised the therapeutic benefits of dual therapy (median survival 10 d vs. 17 d). Interestingly, the survival benefit of dual therapy with anti–CSF-1 was comparable to that of cediranib monotherapy (Fig. S10), demonstrating that the additional survival benefit seen with dual therapy over cediranib monotherapy is mediated mainly by TAMs.

Discussion

Here we report that combined inhibition of VEGFRs and Ang-2 significantly improves survival over monotherapy arms in murine GBM models. Dual therapy improved the extent of vascular normalization in two models of GBM, effectively reducing edema to a similar extent as cediranib monotherapy. Dual therapy delayed tumor growth in Gl261 tumors and increased tumor necrosis in U87 tumors. In the murine Gl261 model in immunocompetent mice, Ang-2/VEGFR blockade showed differential impacts on TAM recruitment and polarization. Further, blockade of TAM recruitment by an anti–CSF-1 antibody compromised the survival benefit of dual therapy to a level similar to that of cediranib monotherapy.

Our findings are consistent with previous preclinical reports of combined VEGF and Ang-2 signaling inhibition in various s.c. and orthotopic non-CNS tumor models (34, 36–41). However, in contrast to non-CNS models (34, 36, 38, 42–46), we observed little survival benefit of anti–Ang-2 monotherapy in GBM models. This result may reflect the greater dependence of GBM angiogenesis on VEGF. We show that Ang-2 inhibition alone leads to a modest improvement in vascular normalization and has no additional effect on intracranial edema or tumor growth. Additionally, in U87 tumors the ectopic overexpression of Ang-2 has little effect on the tumor vasculature or survival but is able to impair the normalization induced by blocking VEGF signaling (27). These data suggest that Ang-2 may be more relevant as a therapeutic target in GBM in the context of VEGF pathway inhibition.

Previously we have shown that the inhibition of VEGF during tumor growth leads to vascular normalization, the extent of which was associated with survival in preclinical models (10, 11, 27) and GBM patients (47–50). Recent clinical data suggest that improved tumor perfusion and oxygenation in both newly diagnosed and rGBM patients during anti-VEGF therapy correlates with significantly longer survival than seen in patients whose tumor blood perfusion does not increase or decreases (47–50). In both U87 and Gl261 tumors dual therapy resulted in a vasculature that more closely resembled that of the surrounding brain. In Gl261 tumors this effect occurred without a reduction in MVD, whereas the more vascularized U87 model required a reduction in MVD to attain the same end point

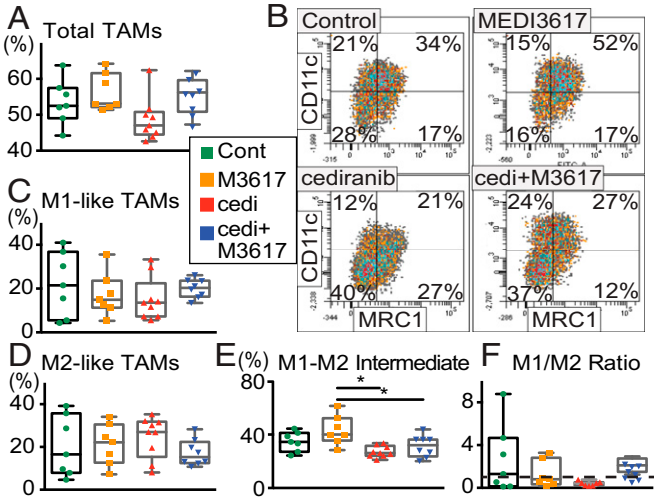

Fig. 5. Cediranib and MEDI3617 have differential effects on TAM recruitment and polarization in Gl261 tumors. Immune cell profiles in Gl261 tumors were analyzed by flow cytometry on day 10. (*A*) The percentage of F4/80$^+$ TAMs was significantly different among treatment groups (ANOVA $P = 0.046$; $n = 7$ or 8). Cediranib monotherapy tended to reduce the percentage of TAMs compared with MEDI3617 monotherapy and dual therapy ($P = 0.054$ and $P = 0.096$, respectively). (*B*) Representative images of the gating strategy to define TAM phenotypes for each treatment group. TAMs were defined as one of four phenotypes: M1-like TAM (CD11c$^+$MRC1$^-$), M2-like (CD11c$^-$MRC1$^+$), M1–M2 intermediate (CD11c$^+$MRC1$^+$), and double-negative (CD11c$^-$MRC1$^-$) TAMs. (*C*) There was no significant difference among treatment groups in the percentage of M1-like TAMs. (*D*) There was no significant difference among any of the groups in the percentage of M2-like TAMs. (*E*) There was a significant difference among treatment groups in the percentage of M1–M2 intermediate TAMs that did not display clear M1- or M2-like activation (ANOVA $P = 0.0031$). Furthermore, both cediranib monotherapy and dual therapy significantly reduced the percentage of these TAMs compared with MEDI3617 monotherapy (*$P = 0.0019$ and *$P = 0.029$). (*F*) There was a trend toward a difference among treatment groups in the M1/M2 ratio (Kruskal–Wallis test, $P = 0.098$). Dual therapy tended to increase M1/M2 ratio compared with cediranib monotherapy ($P = 0.053$). The dashed line indicates an M1/M2 ratio of 1. Total TAMs were normalized to CD45$^+$ cells for comparisons among treatment groups. All TAM phenotypes described were normalized to total F4/80$^+$ cells for comparisons among treatment groups. Error bars represent the SEM.

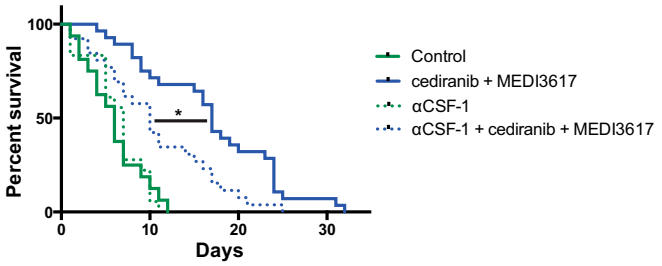

Fig. 6. Inhibition of macrophage recruitment by CSF-1 blockade compromises the survival benefit of dual cediranib+MEDI3617 therapy. Mice bearing GI261 tumors were treated with control ($n = 16$; solid green trace), anti–CSF-1 (αCSF-1; $n = 18$; dotted green trace), dual cediranib+MEDI3617 therapy ($n = 28$; solid blue trace), or anti–CSF-1 + dual therapy ($n = 26$; dotted blue trace). Anti–CSF-1 by itself had no effect on overall median survival compared with control treatment (7 d vs. 6 d). When combined with dual therapy, however, anti–CSF-1 significantly reduced overall median survival compared with dual therapy alone (10 d vs. 17 d; $^*P = 0.003$). Dual therapy with or without combined anti–CSF-1 treatment significantly increased overall median survival compared with control treatment ($P = 0.0035$ and $P < 0.0001$, respectively). These data confirm the role of macrophages as essential mediators of the survival benefits observed with dual therapy.

(i.e., ~300 vessels/mm^2). The resulting extension of vascular normalization beyond that of cediranib monotherapy warrants further studies in combination with radiation, chemotherapy, or immunotherapy, because improvements in the tumor vasculature often improve the delivery and efficacy of other therapeutics (15).

Vascular normalization can enhance the influx of immune effector cells into tumors and prolong the survival of tumor-bearing mice receiving active immunotherapy (15, 51). TAM infiltration is an important determinant of tumor progression and response to therapy in GBM and other tumors (31–33). TAMs may be activated and polarized within a continuum of phenotypes, of which M1 and M2 macrophages represent two extreme phenotypes, depending on the specific cytokines and growth factors produced in the tumor microenvironment. CD11c and MRC1 are commonly used to identify M1- and M2-like TAMs, respectively (52). In many malignant tumor settings, including GBM, TAMs are skewed toward a protumoral M2-like phenotype and promote tumor angiogenesis and progression through the secretion of molecules such as VEGF and MMP-9 (32, 53–60). Both MEDI3617-treated tumors ($P = 0.054$) and dual therapy-treated tumors ($P = 0.096$) exhibited a trend toward increased TAMs compared with cediranib-treated tumors (Fig. 5*A*). These data suggest that the direct effects of blocking VEGFR or Tie-2 signaling in TAMs and the indirect effects via antivascular effects on immune cell populations are potentially independent. Furthermore, there was a trend toward a higher M1/M2 ratio in tumors treated with dual therapy than in tumors treated with cediranib alone (Kruskal–Wallis $P = 0.098$; $P = 0.053$ between the cediranib and dual-therapy arms) (Fig. 5*E*), suggesting that dual therapy may shift the balance of TAMs toward an antitumor phenotype. This observation is further supported by data in our companion paper showing that simultaneous blockade of Ang-2 and VEGF using a bispecific antibody significantly induces M1-like TAM polarization and increases the M1/M2 ratio compared with VEGF-inhibition alone in vivo (61).

We also found that the majority of TAMs did not show clear M1- or M2-like activation and that the proportion of these cells was significantly altered after dual therapy. The significance of these populations remains unclear and should be defined in future studies; however, we speculate that they may represent TAMs within the M1–M2 continuum that have the plasticity to differentiate into either protumor or antitumor TAMs depending on the cytokine milieu. In our previous study vascular normalization increased the production of immune-stimulatory factors while also reducing immune-suppressive factors in TAMs compared with control-treated tumors (30). Because dual therapy normalizes the vasculature, TAMs in dual therapy-treated tumors are adapted to an antitumor phenotype, as shown in our companion manuscript, and thus are able to affect survival positively. However, additional interventions may be necessary to decrease the MDSCs and further activate cytotoxic T lymphocytes—for example by immune checkpoint inhibition—to enhance antitumor adaptive immunity further (30, 62, 63). Taken together, our data warrant further studies to assess the therapeutic potential of the anti-VEGF/Ang-2 combination with novel immunotherapeutics in GBM (51, 64).

Reprogramming the tumor immune environment is a promising therapeutic strategy; preclinical studies blocking TAM function or repolarizing TAMs show promising survival benefits in multiple tumor models (58, 65–67). We previously have shown that anti-VEGF therapy can enhance the recruitment of TAMs in preclinical GBM models and that the number of TAMs is negatively correlated with survival in GBM patients, confirming their potential as a therapeutic target in GBM (11, 68). A recent preclinical study in GBM found that survival could be enhanced by shifting the TAM phenotype away from an M2-like phenotype (33). Here we show that dual blockade of Ang-2 and VEGFR leads to improved vascular normalization and tends to alter the TAM phenotype and/or recruitment compared with anti-VEGFR monotherapy. These changes are associated with delayed GBM progression and increased survival. This dual targeting approach may be an effective way to overcome the resistance to anti-VEGF monotherapy that develops rapidly in patients with GBM.

Materials and Methods

All animal procedures followed Public Health Service Policy on Humane Care of Laboratory Animals guidelines and were approved by the Massachusetts General Hospital (MGH) Institutional Animal Care and Use Committee. MGH is accredited with the Association for Assessment and Accreditation of Laboratory Animal Care and the NIH Office of Laboratory Animal Welfare (A3596-01).

GI261 and U87 cells were orthotopically implanted into C57BL/6 and nude mice, respectively, and were monitored for tumor growth using intravital fluorescence microscopy or optical frequency domain imaging (OFDI) (69). Treatment with IgG control (10 mg/kg) (MedImmune), MEDI3617 (10 mg/kg), cediranib (6 mg/kg), or dual therapy was initiated at tumor diameters of 2.5 mm in U87 tumors or 2.0 mm in GI261 tumors. MRI was used to determine tumor size at the time points described. Tissue was harvested and frozen or paraffin-embedded for histological analyses. Ki67, cleaved caspase 3, CD31, collagen IV, and desmin stainings were assessed using MATLAB or Image J. Edema was assessed using dry/wet weight analysis (11). Tumors were harvested at day 10 for flow cytometry, stained for TAM markers, and analyzed with FACSDiva (BD Biosciences) or FlowJo (Tree Star) software. Data are expressed as mean ± SEM. The *t* tests were two-sided. For comparisons among more than two groups ANOVA or Kruskal–Wallis tests were followed by post hoc multiple comparisons. $P < 0.05$ was considered significant. Experimental procedures are described in detail in *SI Materials and Methods*.

ACKNOWLEDGMENTS. We thank S. Roberge for outstanding technical support for mouse studies; P. Huang for managing the mouse colony and generating mice for the paper; and E. Ager, S. Goel, and C. Kesler for valuable discussions and experimental assistance. The investigators' research was supported by NIH Grants P01-CA080124 (to R.K.J., D.G.D., and D.F.), P50CA165962 (to T.T.B. and R.K.J.), R01CA126642 and R35CA197743 (to R.K.J.), R01-CA096915 and S10-RR027070 (to D.F.), and R01-CA159258 (to D.G.D.); by National Cancer Institute/Federal Share Proton Beam Program Income (R.K.J. and D.F.); by Department of Defense Breast Cancer Research Innovator Award W81XWH-10-1-0016 (to R.K.J.); by grants from MedImmune and the National Foundation for Cancer Research (to R.K.J.); by a Children's Tumor Foundation (CTF) Clinical Research Award, an American Cancer Society Research Scholar Award, and an Ira Spiro Award (all to L.X.); and by the CTF Drug Discovery Initiative (L.X.). Additional support was provided by German Research Foundation and Solidar-Immun Foundation Fellowships (to J.K.); an Aid for Cancer Research Foundation Fellowship (to Z.A.); a Susan G. Komen Postdoctoral Fellowship (to G.S.); a Tosteson & Fund for Medical Discovery Fellowship (to T.V.); Affymetrix (M.S.); a CTF Clinical Research Award, an American Cancer Society Research Scholar Award, and an Ira Spiro Award (all to L.X.); and the CTF Drug Discovery Initiative (L.X.).

1. Lu-Emerson C, et al. (2015) Lessons from anti-vascular endothelial growth factor and anti-vascular endothelial growth factor receptor trials in patients with glioblastoma. *J Clin Oncol* 33(10):1197–1213.
2. Friedman HS, et al. (2009) Bevacizumab alone and in combination with irinotecan in recurrent glioblastoma. *J Clin Oncol* 27(28):4733–4740.
3. Kreisl TN, et al. (2009) Phase II trial of single-agent bevacizumab followed by bevacizumab plus irinotecan at tumor progression in recurrent glioblastoma. *J Clin Oncol* 27(5):740–745.
4. Vredenburgh JJ, et al. (2007) Phase II trial of bevacizumab and irinotecan in recurrent malignant glioma. *Clin Cancer Res* 13(4):1253–1259.
5. Vredenburgh JJ, et al. (2007) Bevacizumab plus irinotecan in recurrent glioblastoma multiforme. *J Clin Oncol* 25(30):4722–4729.
6. Chinot OL, et al. (2014) Bevacizumab plus radiotherapy-temozolomide for newly diagnosed glioblastoma. *N Engl J Med* 370(8):709–722.
7. Gilbert MR, et al. (2014) A randomized trial of bevacizumab for newly diagnosed glioblastoma. *N Engl J Med* 370(8):699–708.
8. Wick W, et al. (2015) LB-05 phase III trial exploring the combination of bevacizumab and lomustine in patients with first recurrence of a glioblastoma: The EORTC 26101 trial. *Neuro-oncol* 17(Suppl 5):v1.
9. Batchelor TT, et al. (2013) Phase III randomized trial comparing the efficacy of cediranib as monotherapy, and in combination with lomustine, versus lomustine alone in patients with recurrent glioblastoma. *J Clin Oncol* 31(26):3212–3218.
10. Winkler F, et al. (2004) Kinetics of vascular normalization by VEGFR2 blockade governs brain tumor response to radiation: Role of oxygenation, angiopoietin-1, and matrix metalloproteinases. *Cancer Cell* 6(6):553–563.
11. Kamoun WS, et al. (2009) Edema control by cediranib, a vascular endothelial growth factor receptor-targeted kinase inhibitor, prolongs survival despite persistent brain tumor growth in mice. *J Clin Oncol* 27(15):2542–2552.
12. Batchelor TT, et al. (2010) Phase II study of cediranib, an oral pan-vascular endothelial growth factor receptor tyrosine kinase inhibitor, in patients with recurrent glioblastoma. *J Clin Oncol* 28(17):2817–2823.
13. Batchelor TT, et al. (2007) AZD2171, a pan-VEGF receptor tyrosine kinase inhibitor, normalizes tumor vasculature and alleviates edema in glioblastoma patients. *Cancer Cell* 11(1):83–95.
14. Jain RK (2005) Normalization of tumor vasculature: An emerging concept in antiangiogenic therapy. *Science* 307(5706):58–62.
15. Jain RK (2014) Antiangiogenesis strategies revisited: From starving tumors to alleviating hypoxia. *Cancer Cell* 26(5):605–622.
16. Carmeliet P, Jain RK (2011) Molecular mechanisms and clinical applications of 6angiogenesis. *Nature* 473(7347):298–307.
17. Holash J, Wiegand SJ, Yancopoulos GD (1999) New model of tumor angiogenesis: Dynamic balance between vessel regression and growth mediated by angiopoietins and VEGF. *Oncogene* 18(38):5356–5362.
18. Hu B, et al. (2003) Angiopoietin-2 induces human glioma invasion through the activation of matrix metalloprotease-2. *Proc Natl Acad Sci USA* 100(15):8904–8909.
19. Lee OH, et al. (2006) Sustained angiopoietin-2 expression disrupts vessel formation and inhibits glioma growth. *Neoplasia* 8(5):419–428.
20. Stratmann A, Risau W, Plate KH (1998) Cell type-specific expression of angiopoietin-1 and angiopoietin-2 suggests a role in glioblastoma angiogenesis. *Am J Pathol* 153(5): 1459–1466.
21. Zagzag D, et al. (1999) In situ expression of angiopoietins in astrocytomas identifies angiopoietin-2 as an early marker of tumor angiogenesis. *Exp Neurol* 159(2):391–400.
22. Hu B, Cheng SY (2009) Angiopoietin-2: Development of inhibitors for cancer therapy. *Curr Oncol Rep* 11(2):111–116.
23. Daly C, et al. (2006) Angiopoietin-2 functions as an autocrine protective factor in stressed endothelial cells. *Proc Natl Acad Sci USA* 103(42):15491–15496.
24. Kim I, et al. (2000) Angiopoietin-2 at high concentration can enhance endothelial cell survival through the phosphatidylinositol 3′-kinase/Akt signal transduction pathway. *Oncogene* 19(39):4549–4552.
25. Teichert-Kuliszewska K, et al. (2001) Biological action of angiopoietin-2 in a fibrin matrix model of angiogenesis is associated with activation of Tie2. *Cardiovasc Res* 49(3):659–670.
26. Augustin HG, Koh GY, Thurston G, Alitalo K (2009) Control of vascular morphogenesis and homeostasis through the angiopoietin-Tie system. *Nat Rev Mol Cell Biol* 10(3):165–177.
27. Chae SS, et al. (2010) Angiopoietin-2 interferes with anti-VEGFR2-induced vessel normalization and survival benefit in mice bearing gliomas. *Clin Cancer Res* 16(14): 3618–3627.
28. di Tomaso E, et al. (2011) Glioblastoma recurrence after cediranib therapy in patients: Lack of "rebound" revascularization as mode of escape. *Cancer Res* 71(1):19–28.
29. Sie M, et al. (2009) The angiopoietin 1/angiopoietin 2 balance as a prognostic marker in primary glioblastoma multiforme. *J Neurosurg* 110(1):147–155.
30. Huang Y, et al. (2012) Vascular normalizing doses of antiangiogenic treatment reprogram the immunosuppressive tumor microenvironment and enhance immunotherapy. *Proc Natl Acad Sci USA* 109(43):17561–17566.
31. Qian BZ, Pollard JW (2010) Macrophage diversity enhances tumor progression and metastasis. *Cell* 141(1):39–51.
32. Mantovani A, Sica A (2010) Macrophages, innate immunity and cancer: Balance, tolerance, and diversity. *Curr Opin Immunol* 22(2):231–237.
33. Pyonteck SM, et al. (2013) CSF-1R inhibition alters macrophage polarization and blocks glioma progression. *Nat Med* 19(10):1264–1272.
34. Leow CC, et al. (2012) MEDI3617, a human anti-angiopoietin 2 monoclonal antibody, inhibits angiogenesis and tumor growth in human tumor xenograft models. *Int J Oncol* 40(5):1321–1330.
35. Grenga I, Kwilas AR, Donahue RN, Farsaci B, Hodge JW (2015) Inhibition of the angiopoietin/Tie2 axis induces immunogenic modulation, which sensitizes human tumor cells to immune attack. *J Immunother Cancer* 3:52.
36. Hashizume H, et al. (2010) Complementary actions of inhibitors of angiopoietin-2 and VEGF on tumor angiogenesis and growth. *Cancer Res* 70(6):2213–2223.
37. Koh YJ, et al. (2010) Double antiangiogenic protein, DAAP, targeting VEGF-A and angiopoietins in tumor angiogenesis, metastasis, and vascular leakage. *Cancer Cell* 18(2):171–184.
38. Brown JL, et al. (2010) A human monoclonal anti-ANG2 antibody leads to broad antitumor activity in combination with VEGF inhibitors and chemotherapy agents in preclinical models. *Mol Cancer Ther* 9(1):145–156.
39. Daly C, et al. (2013) Angiopoietin-2 functions as a Tie2 agonist in tumor models, where it limits the effects of VEGF inhibition. *Cancer Res* 73(1):108–118.
40. Kienast Y, et al. (2013) Ang-2-VEGF-A CrossMab, a novel bispecific human IgG1 antibody blocking VEGF-A and Ang-2 functions simultaneously, mediates potent antitumor, antiangiogenic, and antimetastatic efficacy. *Clin Cancer Res* 19(24):6730–6740.
41. Keskin D, et al. (2015) Targeting vascular pericytes in hypoxic tumors increases lung metastasis via angiopoietin-2. *Cell Reports* 10(7):1066–1081.
42. Huang H, et al. (2011) Specifically targeting angiopoietin-2 inhibits angiogenesis, Tie2-expressing monocyte infiltration, and tumor growth. *Clin Cancer Res* 17(5):1001–1011.
43. Oliner J, et al. (2004) Suppression of angiogenesis and tumor growth by selective inhibition of angiopoietin-2. *Cancer Cell* 6(5):507–516.
44. Falcón BL, et al. (2009) Contrasting actions of selective inhibitors of angiopoietin-1 and angiopoietin-2 on the normalization of tumor blood vessels. *Am J Pathol* 175(5):2159–2170.
45. Holopainen T, et al. (2012) Effects of angiopoietin-2-blocking antibody on endothelial cell-cell junctions and lung metastasis. *J Natl Cancer Inst* 104(6):461–475.
46. Mazzieri R, et al. (2011) Targeting the ANG2/TIE2 axis inhibits tumor growth and metastasis by impairing angiogenesis and disabling rebounds of proangiogenic myeloid cells. *Cancer Cell* 19(4):512–526.
47. Sorensen AG, et al. (2012) Increased survival of glioblastoma patients who respond to antiangiogenic therapy with elevated blood perfusion. *Cancer Res* 72(2):402–407.
48. Gerstner ER, Batchelor TT (2012) Antiangiogenic therapy for glioblastoma. *Cancer J* 18(1):45–50.
49. Emblem KE, et al. (2013) Vessel architectural imaging identifies cancer patient responders to anti-angiogenic therapy. *Nat Med* 19(9):1178–1183.
50. Batchelor TT, et al. (2013) Improved tumor oxygenation and survival in glioblastoma patients who show increased blood perfusion after cediranib and chemoradiation. *Proc Natl Acad Sci USA* 110(47):19059–19064.
51. Kwilas AR, Donahue RN, Tsang KY, Hodge JW (2015) Immune consequences of tyrosine kinase inhibitors that synergize with cancer immunotherapy. *Cancer Cell Microenviron* 2(1):e677.
52. Mantovani A, Allavena P (2015) The interaction of anticancer therapies with tumor-associated macrophages. *J Exp Med* 212(4):435–445.
53. Solinas G, Germano G, Mantovani A, Allavena P (2009) Tumor-associated macrophages (TAM) as major players of the cancer-related inflammation. *J Leukoc Biol* 86(5):1065–1073.
54. De Palma M, Naldini L (2006) Role of haematopoietic cells and endothelial progenitors in tumour angiogenesis. *Biochim Biophys Acta* 1766(1):159–166.
55. Lewis JS, Landers RJ, Underwood JC, Harris AL, Lewis CE (2000) Expression of vascular endothelial growth factor by macrophages is up-regulated in poorly vascularized areas of breast carcinomas. *J Pathol* 192(2):150–158.
56. Lin EY, et al. (2006) Macrophages regulate the angiogenic switch in a mouse model of breast cancer. *Cancer Res* 66(23):11238–11246.
57. Hanahan D, Coussens LM (2012) Accessories to the crime: Functions of cells recruited to the tumor microenvironment. *Cancer Cell* 21(3):309–322.
58. DeNardo DG, et al. (2011) Leukocyte complexity predicts breast cancer survival and functionally regulates response to chemotherapy. *Cancer Discov* 1(1):54–67.
59. Komohara Y, Ohnishi K, Kuratsu J, Takeya M (2008) Possible involvement of the M2 anti-inflammatory macrophage phenotype in growth of human gliomas. *J Pathol* 216(1):15–24.
60. Noy R, Pollard JW (2014) Tumor-associated macrophages: From mechanisms to therapy. *Immunity* 41(1):49–61.
61. Kloepper J, et al. (2016) Ang-2/VEGF bispecific antibody reprograms macrophages and resident microglia to anti-tumor phenotype and prolongs glioblastoma survival. *Proc Natl Acad Sci USA* 113:4476–4481.
62. Yasuda S, et al. (2013) Simultaneous blockade of programmed death 1 and vascular endothelial growth factor receptor 2 (VEGFR2) induces synergistic anti-tumour effect in vivo. *Clin Exp Immunol* 172(3):500–506.
63. Hamzah J, et al. (2008) Vascular normalization in Rgs5-deficient tumours promotes immune destruction. *Nature* 453(7193):410–414.
64. Meisen WH, et al. (2015) The Impact of Macrophage- and Microglia-Secreted TNFα on Oncolytic HSV-1 Therapy in the Glioblastoma Tumor Microenvironment. *Clin Cancer Res* 21(14):3274–3285.
65. Stockmann C, et al. (2008) Deletion of vascular endothelial growth factor in myeloid cells accelerates tumorigenesis. *Nature* 456(7223):814–818.
66. Beatty GL, et al. (2011) CD40 agonists alter tumor stroma and show efficacy against pancreatic carcinoma in mice and humans. *Science* 331(6024):1612–1616.
67. De Palma M, et al. (2008) Tumor-targeted interferon-alpha delivery by Tie2-expressing monocytes inhibits tumor growth and metastasis. *Cancer Cell* 14(4):299–311.
68. Lu-Emerson C, et al. (2013) Increase in tumor-associated macrophages after antiangiogenic therapy is associated with poor survival among patients with recurrent glioblastoma. *Neuro-oncol* 15(8):1079–1087.
69. Vakoc BJ, et al. (2009) Three-dimensional microscopy of the tumor microenvironment in vivo using optical frequency domain imaging. *Nat Med* 15(10):1219–1223.
70. Yuan F, et al. (1994) Vascular permeability and microcirculation of gliomas and mammary carcinomas transplanted in rat and mouse cranial windows. *Cancer Res* 54(17):4564–4568.
71. Xu L, Xie K, Fidler IJ (1998) Therapy of human ovarian cancer by transfection with the murine interferon beta gene: Role of macrophage-inducible nitric oxide synthase. *Hum Gene Ther* 9(18):2699–2708.